Current-induced Breakdown of Carbon Nanofibers

Under Vacuum and Atmospheric Conditions

H. Kitsuki[*], Q. Ngo[*,**], M. Suzuki[*], K. Gleason[*], P. Wilhite[*], A. M. Cassell[**], C. R. Moylan[***], J. Li[**] and C. Y. Yang[*]

[*] Center for Nanostructures, Santa Clara University, Santa Clara, California

[**] Center for Advanced Aerospace Materials and Devices, NASA Ames Research Center, Moffett Field, California

[***] Department of Electrical Engineering, University of California-Santa Cruz, Santa Cruz, California

ABSTRACT

Current-induced breakdown phenomena of carbon nanofibers (CNFs) for the development of carbon-based interconnects are investigated to reveal current-carrying capacity and reliability of CNF devices. Scanning transmission electron microscopy (STEM) techniques are developed to study the structural damage by current stress, including in-situ electrical measurement in STEM. The correlation between maximum current density and electrical resistivity confirms the importance of local Joule heating, showing strong coupling between electrical and thermal transport in CNFs.

Keywords: carbon nanofibers, current-induced breakdown, scanning transmission electron microscopy (STEM), thermal transport

1 INTRODUCTION

Carbon nanostructures including carbon nanotubes (CNTs) and carbon nanofibers (CNFs) have recently been explored as interconnects for integrated circuit applications [1-5] because of their chemically stable nature and high electrical and thermal conductivities. While CNTs have been well studied as an interconnect material, recent investigations reveal that lower growth temperature [6,7] and better directional control [1] have been achieved in CNFs, which are critical for realistic device fabrication processes.

With regards to their current capacity, comprehensive studies in CNT systems have revealed unique high-field transport properties in single-walled CNTs [8,9] and successive graphitic wall breakdown in multi-walled CNTs [10-12]. For CNF systems, we have recently reported the high-field transport properties [13], demonstrating the high-current reliability of a CNF via structure embedded in an oxide matrix for on-chip interconnects. However, the failure mode of CNFs due to excess current and the accompanying physical mechanisms still remain to be investigated. Since atomic-scale imaging using STEM shows that CNFs consist of cup-shaped graphitic layers stacked along the fiber axis [14-16], structural damage caused by high current stress is likely different from that of CNTs.

In this work, we extend the application-driven development of carbon-based interconnects through a detailed investigation of current-carrying capacity and reliability of CNF. Based on detailed characterization using in situ STEM before, during, and after current-induced breakdown of the device, we propose a model for current-induced breakdown in CNF structures. We also discuss the role of local Joule heating in the breakdown process.

2 EXPERIMENT

The CNF samples are grown by plasma-enhanced chemical vapor deposition (PECVD) [17,18] with Ni catalyst layer on Si substrate. A 30 nm-thick Ti adhesion layer is used between a 35-nm-thick Ni layer and Si. A gas mixture of NH_3:C_2H_2 (4:1) at 4 Torr is used for the reaction. The detailed growth conditions have been described elsewhere [19]. Electrical measurements with concurrent STEM imaging are carried out in a field-emission scanning electron microscope (SEM, Hitachi S-4800) with STEM capability using an electron beam energy of 30 keV.

Figure 1 illustrates our STEM imaging techniques for the current-induced breakdown of CNF. To investigate the detailed failure mechanism, a suspended CNF device structure between two electrodes is realized in the STEM specimen chamber under a vacuum of 10^{-5} Torr [Fig. 1(a)]. An external current source is connected to these electrodes, enabling in situ imaging during current stressing. In order to study the failure mode of the CNFs fabricated in a more realistic device structure on a Si substrate, a STEM imaging technique utilizing the reflected signal from a highly-tilted substrate with conventional SEM is also developed [Fig. 1(b)].

Figure 2 shows SEM images of CNF devices for the breakdown experiment. In Fig. 2(a), a CNF is suspended between aluminum and tungsten electrodes. Another CNF is prepared on SiO_2-covered Si substrate with pre-patterned gold pads as shown in Fig. 2(b).

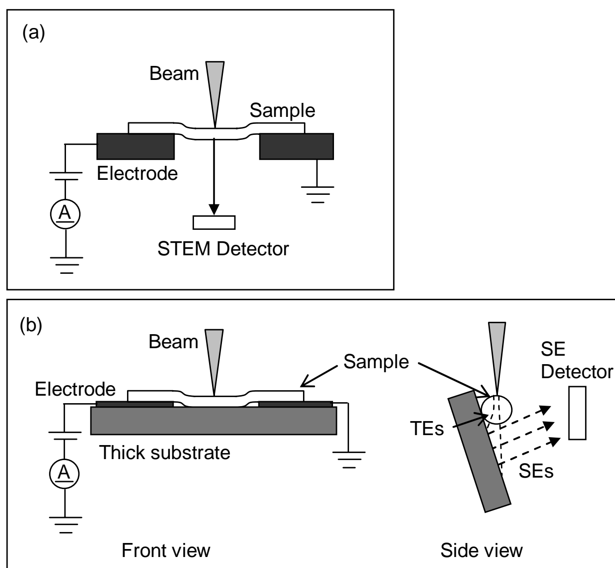

Figure 1: STEM imaging techniques for CNFs (a) suspended between electrodes and (b) placed on a silicon substrate with pre-patterned electrodes.

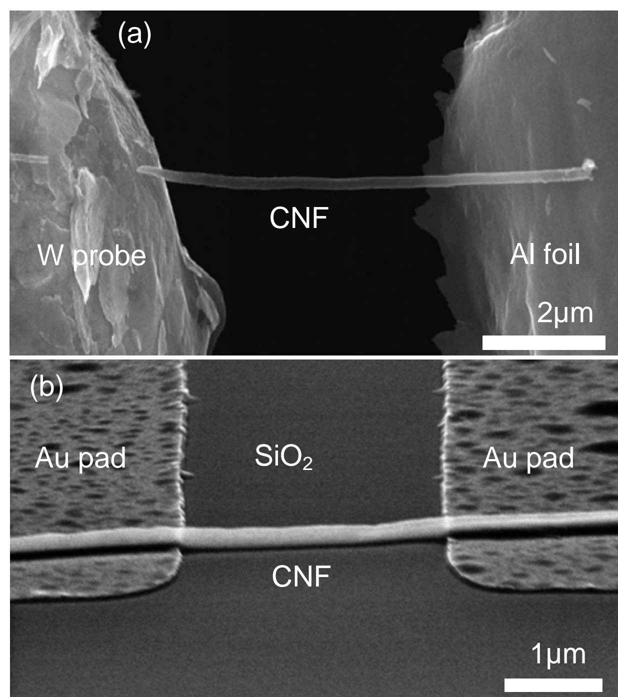

Figure 2. SEM images of device configurations for (a) suspended CNF and (b) on-substrate CNF for breakdown experiments.

3 RESULTS AND DISCUSSION

The breakdown experiments are performed for more than 10 samples in each of the device configurations in Fig. 2 (a) and (b), respectively, and the resulting maximum current before failure ranges from 400 to 1000 μA resulting in maximum current densities from 1×10^6 to 1×10^7 A/cm^2. The average maximum current and current density are 670 μA and 4×10^6 A/cm^2, respectively.

Figure 3(a) shows a typical *I-V* curve for breakdown measurements. Current (*I*) monotonically increases with applied voltage (*V*), and abruptly goes to zero at the current-induced breakdown, exhibiting clear contrast to the case of CNTs, where a stepwise decrease of current is observed [10-12] due to successive CNT shell breakdown in multi-wall CNTs. In Fig. 3(b), STEM images of a suspended CNF after current stress is shown. By applying current through the CNF, breakdown occurs near the mid-point. The mid-point breakdown is consistent with diffusive transport observed in CNTs at a high bias [11]. Damage is typically found between the ordered, cup-shaped layers of graphite, indicating weak interlayer bonding. Diameter thinning is also confirmed, which suggests some of the graphitic layers have oxidized with residual oxygen or vaporized.

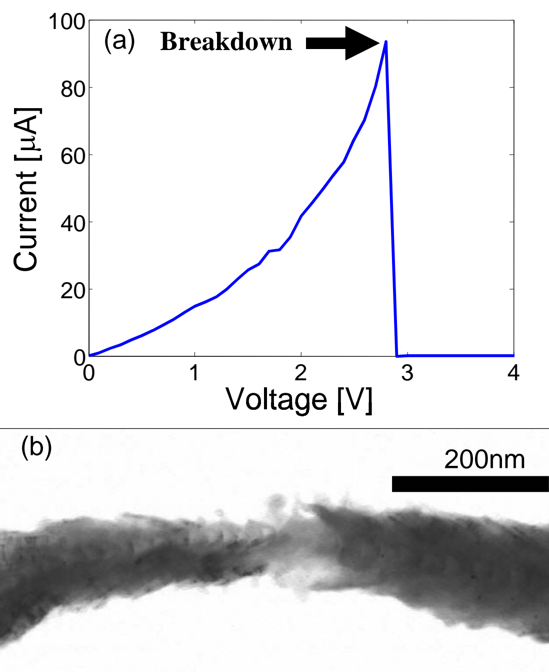

Figure 3 (a) I-V trace of the current-induced breakdown. (b) Typical STEM image of a failed CNF suspended between two electrodes.

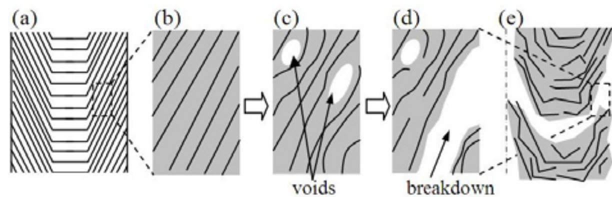

Figure 4. Schematic drawings of CNF breakdown. (a) and (b) Undamaged CNF. (c) Damaged cups creating voids between cups. (d) and (e) Failed CNF after high current stress.

Based on these findings, we propose a CNF breakdown mechanism due to high stress as shown in Fig. 4. By applying current along the cup-shaped CNF, the rigidly stacked graphitic layers start to partially separate, forming a defective fiber with voids (Fig. 4 (c)). Finally, the CNF fails (see Figs. 4 (d) and (e)) as a result of voids and inter-layer breakdown.

Using the device configuration in atmospheric condition as shown in Fig. 1(b), electrical breakdown has been performed for 12 different CNFs on an oxidized silicon substrate. STEM images of a CNF before and after breakdown are shown in Figs 5(a) and (b), respectively. Utilizing the technique shown in Fig. 1(b), internal structural change due to high-current stress is observed. Contrary to the case of suspended CNFs discussed in Fig. 3(b), a typical CNF shows structural change in the form of an internal void region (bright area) inside the fiber. This indicates the effect of the substrate is significant in the breakdown process.

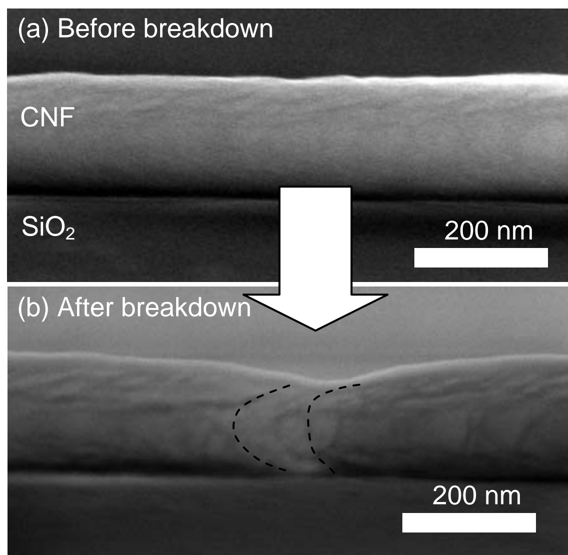

Figure 5. STEM images of a CNF on oxidized silicon substrate before and after breakdown are shown in (a) and (b), respectively.

Figure 6 shows the relationship between maximum current density and CNF diameter for 12 samples suspended between two electrodes. From the samples characterized, it is difficult to discern a pattern for maximum current density or even a correlation with diameter. This result implies non-uniformity of internal morphology of CNFs caused by current-induced divergence of graphitic layers or evaporation, and suggests effective resistivity should dominate maximum current as discussed below.

Figure 7 shows the correlation between breakdown current density and electrical resistivity. Data for suspended CNFs [Fig. 2(a)] are given by solid circles. A power-law correlation between resistivity and maximum current density is observed, implying that CNFs with higher resistivity are more prone to failure even at the same generated heat [20], possibly due to higher structural defect density of the CNF with higher electrical resistivity. This correlation also indicates the importance of resistive Joule heating [21] to the CNF breakdown process [22].

The effective heat dissipation by the surrounding materials and ambient, as well as lowering electrical resistivity, is expected to improve the nanofiber's current transport capacity. The dependence of the maximum current density on resistivity observed for the on-substrate configuration [Fig. 2(b)] is plotted with open circles in Fig. 7, representing a similar power-law dependence as the suspended case with slightly improved current carrying capacity (i.e. higher maximum current density). This result indicates that heat dissipation via its immediate surroundings critically affects high-current transport in the CNF.

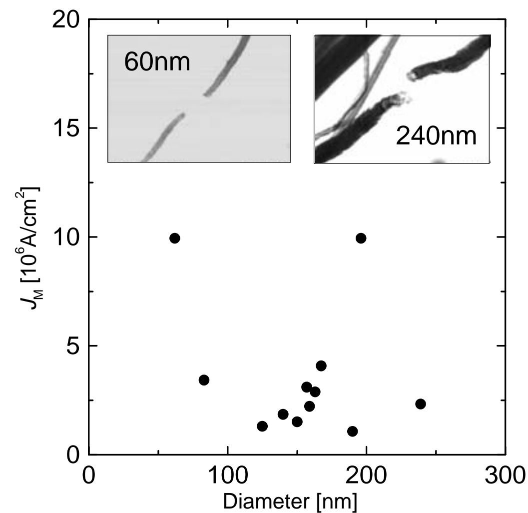

Figure 6. Breakdown current density versus diameter. No clear correlation between J_M and diameter is observed.

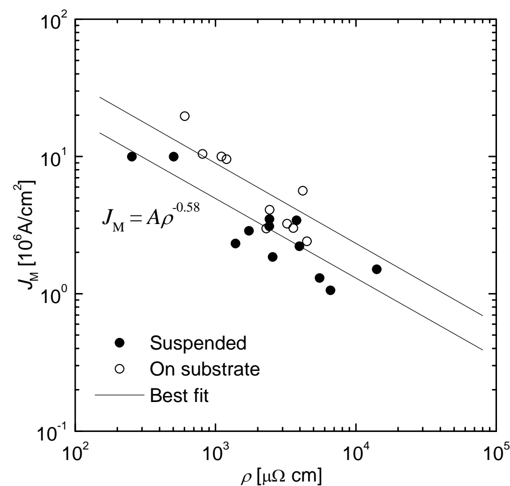

Figure 7. Correlation of breakdown current density to resistivity for suspended CNF measurements and on-substrate CNF measurements. The best-fit (solid) lines show a power law dependence in each case.

NSTI-Nanotech 2007, www.nsti.org, ISBN 1420061828 Vol. 1, 2007

CONCLUSION

The study of CNF breakdown caused by high-current stress has been performed using two distinct geometrical configurations. In-situ STEM imaging techniques enable us to obtain detailed structural change information due to current stress, indicating that the breakdown occurs at the weak inter-layer bonding between graphitic layers comprising the CNF. The correlation between maximum current density and electrical resistivity implies that local Joule heating is responsible for the breakdown phenomena of CNFs. This study demonstrates an important advance in failure analysis of carbon-based nanostructures for development of future interconnect applications.

ACKNOWLEDGMENTS

The authors are grateful to Kevin Mcllwrath and Konrad Jarausch of Hitachi High-Technologies America, Inc. for their expert technical support for our STEM experiments.

REFERENCES

[1] J. Li, Q. Ye, A. Cassell, H. T. Ng, R. Stevens, J. Han, and M. Meyyappan, Appl. Phys. Lett. 82, 2491 (2003).
[2] F. Kreupl, A. P. Graham, M. Liebau, G. S. Duesberg, R. Seidel, E. Unger, International Electron Devices Meeting Technical Digest, pp. 683-686, San Francisco, CA, 2004.
[3] S. Sato, M. Nihei, A. Mimura, A. Kawabata, D. Kondo, H. Shioya, T. Iwai, M. Mishima, M. Ofuti, and Y. Awano, Proc. of the IEEE 2006 Int. Interconnect Technol. Conf., pp. 230-232, San Francisco, CA, 2006.
[4] Y.-M. Choi, S. Lee, H. S. Yoon, M.-S. Lee, H. Kim, I. Han, Y. Son, I.-S. Yeo, U.-I. Chung, J.-T. Moon, Proc. of 6th IEEE NANO Conf., Vol. 1, pp-262-265, Cincinnati, OH, 2006.
[5] L. Dong, S. Youkey, J. Bush, J. Jiao, V. M. Dubin, R. V. Chebiam, J. Appl. Phys. 101, 024320 (2007).
[6] B. O. Boskovic, V. Stolojan, R. U. A. Khan, S. Haq, and S. R. P. Silva, Nature Mater. 1, 165-168 (2002).
[7] S. Hofmann, C. Ducati, B. Kleinsorge, and J. Robertson, Appl. Phys. Lett. 83, 4661 (2003).
[8] Z. Yao, C. L. Kane, and C. Dekker, Phys. Rev. Lett 84, 2941 (2000).
[9] A. Javey, J. Guo, M. Paulsson, Q. Wang, D. Mann, M. Lundstrom, and H. Dai, Phys. Rev. Lett. 92, 106804 (2004).
[10] P. G. Collins, M. Hersam, M. Arnold, R. Martel, and Ph. Avouris, Phys. Rev. Lett. 86, 3128 (2001).
[11] J. Y. Huang, S. Chen, S. H. Jo, Z. Wang, D. X. Han, G. Chen, M. S. Dresselhaus, and Z. F. Ren, Phys. Rev. Lett. 94, 236802 (2005).
[12] T. D. Yuzvinsky, W. Mickelson, S. Aloni, S. L. Konsek, A. M. Fennimore, G. E. Begtrup, A. Kis, B. C. Regan, and A. Zettl, Appl. Phys. Lett. 87, 083103 (2005).
[13] Q. Ngo, A. M. Cassell, A. J. Austin, J. Li, S. Krishnan, M. Meyyappan, and C. Y. Yang, IEEE Electron Device Lett. 27, 221 (2006).
[14] S. Helveg, C. López-Cartes, J. Sehested, P. L. Hansen, B. S. Clausen, J. R. Rostrup-Nielsen, F. Abild-Pedersen, and J. K. Nørskov, Nature (London) 427 426, (2004).
[15] H. Cui, X. Yang, M. L. Simpson, D. H. Lowndes, and M. Varela, Appl. Phys. Lett. 84, 4077 (2004).
[16] Y. Ominami, Q. Ngo, A. J. Austin, H. Yoong, C. Y. Yang, A. M. Cassell, B. A. Cruden, J. Li, and M. Meyyappan, Appl. Phys. Lett. 87, 233105 (2005).
[17] Y. Chen, Z. L. Wang, J. S. Yin, D. J. Johnson and R. H. Prince, Chem. Phys. Lett. 272, 178 (1997).
[18] Z. F. Ren, Z. P. Huang, J. W. Xu, J. H. Wang, P. Bush, M. P. Siegal, and P. N. Provencio, Science 282, 1105 (1998).
[19] B. A. Cruden, A. M. Cassell, Q. Ye and M. Meyyappan, J. Appl. Phys. 94, 4070 (2003).
[20] M. Suzuki, Y. Ominami, Q. Ngo, A. M. Cassell, J. Li, C. Y. Yang, submitted to J. Appl. Phys.
[21] C. Durkan, M. A. Schneider, and M. E. Welland, J. Appl. Phys. 86, 1280 (1999).
[22] M. A. Kuroda, A. Cangellaris, and J.-P. Leburton, Phys. Rev. Lett. 95, 266803 (2005).